Torque Minimization of Dynamically Decoupled 3R Spatial Serial Manipulators via Optimal Motion Generation

YAODONG LU, VIGEN ARAKELIAN
[1]ECN, LS2N UMR 6004,
1 rue de la Noë, BP 92101, F-44321 Nantes,
FRANCE

also with
[2]Mecaproce / INSA Rennes,
20 av. des Buttes de Coësmes, CS 70839, F-35708 Rennes,
FRANCE

Abstract: - This paper proposes an analytically tractable solution for minimizing input torques in decoupled three-degrees-of-freedom spatial serial manipulators. The solution relies on the generation of motion using a «bang-bang» profile. The problem is solved in two stages. Firstly, the dynamic decoupling of the manipulator is accomplished through the redistribution of the moving masses and the relocation of one of the actuators. This leads to the decoupling of the equations of motion for different degrees of mobility. It is worth mentioning that this solution represents a symbiosis of two distinct approaches: the redistribution of link masses and the relocation of one of the manipulator actuators. This innovative approach to dynamic decoupling has not been previously proposed. At the second stage, the input torques of the actuators are reduced by generating motion profiles for the manipulator's links using the «bang-bang» law. Thus, thanks to the developed methodology, it becomes possible to reduce the energy consumption of high-speed manipulators by choosing the optimal planned motion of their links. To evaluate the effectiveness of this approach, numerical simulations are carried out using the ADAMS software. A comparative analysis of the trajectories generated by the fifth-order polynomial profile, widely used in industrial robots, and the «bang-bang» profile has been performed. The simulation results show act, the use of the «bang-bang» profile allows one to reduce the maximum values of the input torques. The developed technique allows designers to create high-speed manipulators featuring decoupled dynamics and diminished energy consumption.

Key-Words: - Manipulator, dynamics, decoupling, torque, «bang-bang» profile, optimal generation of motions

Received: February 24, 2023. Revised: July 21, 2023. Accepted: August 26, 2023. Published: September 14, 2023.

1 Introduction

It is known that the manipulator dynamics are highly coupled and nonlinear. This complexity arises from various factors such as changing inertia, interactions between different joints, and nonlinear forces like Coriolis and centrifugal forces. The goal of dynamic decoupling in manipulators is to achieve conditions that allow for decoupled and linear dynamic equations. This simplifies optimal control and energy accumulation in manipulators.

Let us consider the classification the methods for dynamic decoupling of manipulators. To achieve a clearer classification, it is convenient to separate them into two levels. Firstly, let us review two different approaches that have been developed for creating dynamically decoupled manipulators: A) by optimal mechanical design and B) by improved control, [1]. There are three main methodologies developed for dynamic decoupling of manipulators via mechanical transformation:

A1) via mass redistribution;
A2) via actuator relocation;
A3) via addition of auxiliary links.

In order to eliminate the coupling and nonlinear torques via mass redistribution (subgroup A1), the inertia matrix must be diagonal and made invariant for all statically balanced arm configurations. These properties were described in detail for various structural solutions in, [2], [3]. Let us explore the essential properties of mass distribution required to achieve this objective.

Let θ_i and τ_i,, be the joint displacement and torque of the i-th joint, respectively, then the equation of motion of the manipulator is given by

$$\tau_i = H_{ii}\ddot{\theta}_i + \sum_{j\neq i} H_{ij}\ddot{\theta}_j + \sum_j \sum_k \left(\partial H_{ij}/\partial\theta_k - \frac{1}{2}\partial H_{jk}/\partial\theta_i\right)\dot{\theta}_j\dot{\theta}_k + \tau_{gi}$$

where, H_{ij} is the *i*-*j* element of the manipulator inertia matrix, and τ_{gi} is the torque due to gravity. The first term in the equation represents the inertia torque resulting from the acceleration of the *i*-th joint, while the second term accounts for the interactive inertia torque arising from the accelerations of the other joints. The interactive inertia torque is directly proportional to the acceleration. The third term captures the nonlinear velocity torques generated by Coriolis and centrifugal effects. These nonlinear velocity torques emerge due to the dependence of the inertia matrix on the arm configuration. However, if the inertia matrix becomes diagonal for any arm configuration, the second term in the aforementioned equation disappears, eliminating the presence of interactive torques. In this case, the manipulator's inertia matrix is referred to as a decoupled inertia matrix. The significance of the decoupled inertia matrix lies in the fact that the control system can be treated as a collection of single-input, single-output subsystems associated with individual joint motions. This decoupling of the inertia matrix enables a simplified control approach, where each joint can be controlled independently without interference from other joints. It facilitates the design and implementation of control strategies for manipula-tors, treating them as separate entities rather than a complex interconnected system.

The equation of motion under these conditions reduces to

$$\tau_i = H_{ii}\ddot{\theta}_i + \sum_k \left(\frac{\partial H_{ii}}{\partial\theta_k}\dot{\theta}_j\dot{\theta}_k - \frac{1}{2}\frac{\partial H_{kk}}{\partial\theta_k}\dot{\theta}_k^2\right) + \tau_{gi}$$

where, the second term represents the nonlinear velocity torques resulting from the spatial dependency of the diagonal elements of the inertia matrix. Note that the number of terms involved in this equation is much smaller than the number of original nonlinear velocity torques, because all the off diagonal elements are zero for $\theta_1, \ldots, \theta_n$. This reduces the computational complexity of the nonlinear torques.

Another important form of the inertia matrix that simplifies the dynamics is a configuration-invariant form. In this case, the inertia matrix remains constant regardless of the arm configuration. This means that it is not dependent on joint displacements, resulting in the elimination of the third term in the first equation mentioned. As a result, the equation of motion reduces to a simplified form

$$\tau_i = H_{ii}\ddot{\theta}_i + \sum_j H_{ij}\ddot{\theta}_j + \tau_{gi}$$

Note that the coefficients H_{ii} and H_{ij} are constant for all arm configurations. Thus, the equation is linear except the last term, that is, the gravity torque. The inertia matrix in this form is referred to as an invariant inertia matrix. The significance of this form is that linear control schemes can be adopted, which are much simpler and easier to implement.

When the inertia matrix is both decoupled and configuration invariant, the equation of motion reduces to:

$$\tau_i = H_{ii}\ddot{\theta}_i + \tau_{gi}$$

The system is completely decoupled and linearized, except the gravity term. Thus, we can treat the system as single-input, single-output systems with constant parameters.

The linearization and dynamic decoupling of 3 degrees of freedom serial manipulators via mass redistribution have been considered, [2]. In this study, all of the arm constructions that yielded the decoupled inertia matrices were identified. The proposed approach is exclusively applied to serial manipulators with non-parallel joint axes. In the case of parallel axes, such an approach allows linearization of the dynamic equations but not their dynamic decoupling, [3].

It should be noted that in the case of planar serial manipulators, the mentioned method cannot be used. Therefore, in serial manipulators with an open kinematic chain structure, the inertia matrix cannot be decoupled unless the joint axes are orthogonal to each other.

Now, let us consider the methods of the sub-group A2. A commonly used arrangement for actuating robot manipulators with motorized joints involves directly attaching motors to the joints. This design does not involve any transmission elements between the actuators and the joints. However, in certain cases, the dynamic decoupling follows from the kinematic decoupling of motion when the rotation of any link is due to only one actuator. It is obvious that it must be accompanied by an optimal choose the mass properties of certain links. It is evident that this must be complemented by an optimal choice of the mass properties of certain links. The optimal selection of mass properties involves carefully determining the distribution of

mass along the manipulator's links. By appropriately choosing the mass distribution, it is possible to achieve improved dynamics and reduce the coupling effects between the joints. This optimization process aims to minimize unwanted interactions between the joints, resulting in more efficient and accurate manipulator performance.

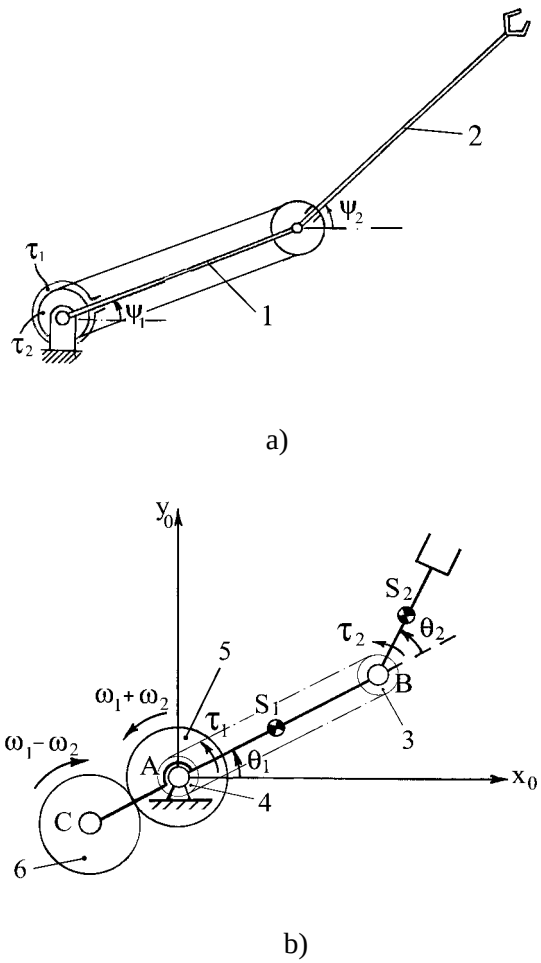

Fig. 1: Dynamic decoupling: via actuator relocation (a) and via addition of auxiliary links (b)

Figure 1a shows such an example, where the actuators are installed at the base of the manipulator and a transmission mechanism is used to rotate the second link. In this case, $\tau_i = H_i\ddot{\psi}_i (i = 1,2)$, with$\psi_1 = \theta_1$ and $\psi_2 = \theta_1 + \theta_2$. In the case of actuating of both joints: θ_1 is the joint displacement of the first link relative to the base; θ_2 is the joint displacement of the second link relative to the first link.

A detailed description of this solution and different structural architectures can be found in, [4], [5], [6], [7], [8], [9], [10], [11].

The linearization of the dynamic equations and their decoupling by adding auxiliary links (subgroup A3) has also been developed, [12], [13], [14], [15]. In this case, the inclusion of complementary links enables the optimal redistribution of kinetic and potential energies, resulting in the linearization and decoupling of the dynamic equations. The process of determining the parameters of these additional links is based on eliminating the coefficients of nonlinear terms present in the manipulator's kinetic and potential energy equations. By carefully selecting and configuring these complementary links, it becomes possible to effectively redistribute the energy within the manipulator system. This redistribution helps to mitigate the nonlinear effects that arise from the interaction between different joints and links. Through a systematic approach, the parameters of the added links can be determined in a way that cancels out or minimizes the coefficients associated with the nonlinear terms in the energy equations. The purpose is to obtain linearized and decoupled dynamic equations, simplifying control and improving performance of the manipulator. By eliminating the nonlinear terms and their coefficients, the dynamics of the system become more predictable and manageable, facilitating the design of efficient control strategies and enhancing the overall functionality of the manipulator. Figure 1b shows such an example, whereby opposite rotation of gears 5 and 6, as well as by an optimal redistribution of mass the dynamic decoupling of the 2 degrees of freedom serial manipulator is achieved.

The design concept of manipulators with adjustable links has been thoroughly investigated in, [15]. This study introduces a novel approach for dynamically decoupling serial planar manipulators by combining mechanical and control solutions. The key idea is to achieve opposite motions of the manipulator links (Figure 2) along with an optimal redistribution of masses. This combination allows for the cancellation of coefficients associated with nonlinear terms in the manipulator's kinetic and potential energy equations. After achieving full linearization and decoupling of the manipulator through this methodology, a linear control technique can be employed. Furthermore, the variation in payload is accounted for by incorporating forward compensation into the controller. To ensure stability of the linearized and decoupled manipulator, a full state feedback control strategy is implemented.

The proposed design concept and control approach offer several advantages. By achieving dynamic decoupling, the manipulator's behavior becomes more predictable and easier to control. The linearized model simplifies control algorithms and allows for the incorporation of compensation techniques to address changing payloads.

Stabilization is ensured through the implementation of a full state feedback loop.

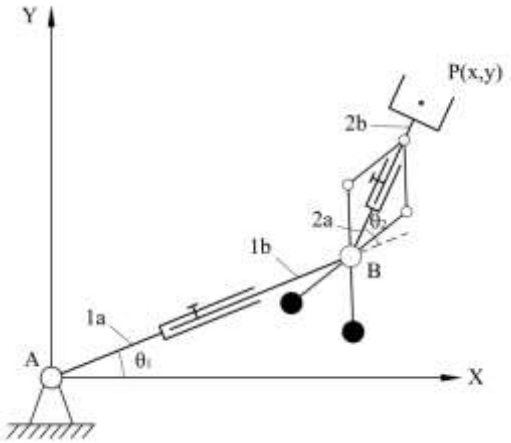

Fig. 2: Dynamic decoupling with adjustable links

This study presents an integrated solution that combines mechanical design considerations with control strategies, resulting in a linearized, decoupled, and stable manipulator system. The results provide insights into the potential benefits and feasibility of this approach for enhancing the performance and control of planar serial manipulators.

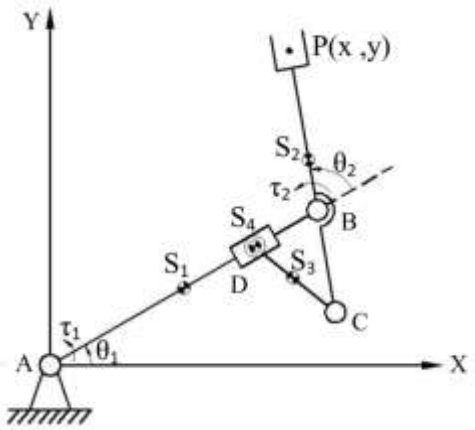

Fig. 3: Two degrees of freedom planar serial manipulator with added two-link group

In, [16], the dynamic decoupling of the manipulator is achieved by introducing a two-link group, forming a Scott-Russell mechanism, to the initial structure. Figure 3 illustrates the robot arm configuration, which consists of two principal links, AB and BP, along with a sub-group comprising links BC and CD. The manipulator's movements are planar motions perpendicular to the vertical plane and, therefore, not subject to gravitational forces in this particular study. The slider D is free to slide along the link AB and is connected to the link CD through a revolute joint D. This arrangement forms a Scott-Russell mechanism when the added sub-group with links BC, CD, and the slider interacts with the link BP of the original structure.

The Scott-Russell mechanism, [17], is known for generating theoretically linear motion by employing a linkage form with three portions of equal-length links and a rolling or sliding connection. In this paper, another property of the mechanism is utilized: it generates rotations of links with identical angular accelerations, meaning that the angular accelerations of links BC and CD are similar. The combination of opposite motion of links within the Scott-Russell mechanism and optimal redistribution of masses enables the cancellation of coefficients associated with nonlinear terms in the manipulator's kinetic and potential energy equations. Subsequently, through optimal control design, dynamic decoupling is achieved, even in the presence of changing payload.

This process becomes relatively straightforward because the modified structure of the manipulator with the two-link group has effectively canceled out coupling and nonlinearity. By utilizing the unique properties of the Scott-Russell mechanism and integrating it into the manipulator structure, this study successfully achieves dynamic decoupling and addresses the impact of changing payloads. The cancellation of coupling and nonlinearity within the modified structure paves the way for easier control and enhanced manipulator performance.

In study, [18], an analysis is presented on the tolerance capabilities of different decoupled models of manipulators. Two indices are proposed to quantify the positioning accuracy of the manipulator: the angular error of the actuators and the position error of the end-effector. To analyze the influence of each variable on the positioning accuracy, fixed parametric errors are introduced. The analysis reveals that the variation in length variables has a higher impact on positioning accuracy compared to other variables. The mass parameters are identified as the second most influential factors, while the inertia parameters have the least influence on positioning accuracy.

Reducing or canceling coupling and nonlinearity in manipulators is often essential, as demonstrated in, [18], [19], [20], [21], [22], [23]. Hence, in this paper, alongside dynamic decoupling, the minimization of input torques is considered.

Torque minimization of dynamically decoupled spatial serial manipulators via optimal motion generation of the 2R spatial serial manipulator has been discussed in, [24]. The problem to be solved was relatively simple, since the dynamic decoupling

of such a manipulator can be carried out by optimal redistribution of moving masses.

The central theme of the present study focuses on torque minimization in dynamically decoupled spatial serial manipulators through optimal motion generation, specifically targeting the 3R spatial serial manipulator. This problem is more complex compared to the previous case, [24]. The present research contributes to enhancing fast manipulator design, allowing for to reduction of the input torques in manipulators with dynamic decoupling.

The next two sections deal with the dynamics of the 3R spatial serial manipulator and the decoupling of its motion equations by mass redistribution and actuator relocating. The combination of these two approaches allows for the elimination of dynamic coupling and non-linearity in 3R spatial manipulators, which improves their performance and control.

2 Dynamics of the Manipulator

The manipulator under consideration consists of three links (Figure 4a): orthogonal links 1 and 2 with rotating angles θ_1, θ_2 and link 3 with rotating angle θ_3, which is parallel to link 2.

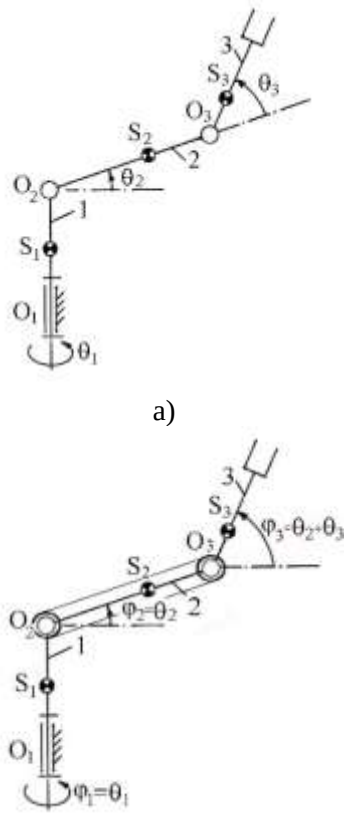

a)

b)

Fig. 4: Spatial serial manipulator: a) initial structure; b) with relocated actuator

We will distinguish the vectors $\dot{\boldsymbol{\theta}}_1^0$, $\dot{\boldsymbol{\theta}}_2^0$ and $\dot{\boldsymbol{\theta}}_3^0$ relative angular velocities with $\dot{\boldsymbol{\theta}}_1^0 = \mathbf{d}\boldsymbol{\theta}_1^0/\mathbf{dt}$, $\dot{\boldsymbol{\theta}}_2 = \mathbf{d}\boldsymbol{\theta}_2^0/\mathbf{dt}$, $\dot{\boldsymbol{\theta}}_3^0 = \mathbf{d}\boldsymbol{\theta}_3^0/\mathbf{dt}$ and the vectors $\dot{\boldsymbol{\theta}}_1$, $\dot{\boldsymbol{\theta}}_2$ and $\dot{\boldsymbol{\theta}}_3$ absolute angular velocities with $\dot{\boldsymbol{\theta}}_1 = \dot{\boldsymbol{\theta}}_1^0$, $\dot{\boldsymbol{\theta}}_2 = \dot{\boldsymbol{\theta}}_1^0 + \dot{\boldsymbol{\theta}}_2^0$ and $\dot{\boldsymbol{\theta}}_3 = \dot{\boldsymbol{\theta}}_1^0 + \dot{\boldsymbol{\theta}}_2^0 + \dot{\boldsymbol{\theta}}_3^0$.

According to Lagrangian dynamics, the equations of motion can be written as:

$$\tau_i = \frac{d}{dt}\left(\frac{\partial L}{\partial \dot{\theta}_i}\right) - \frac{\partial L}{\partial \theta_i},\ i = 1,2,3$$

where, τ_i are the torques; θ_i are the generalized coordinates; $L = K - P$ is the Lagrangian; K is the kinetic energy and P is the potential energy.

The kinetic energy of the manipulator consists of the sum of the kinetic energies of the links: $K = K_1 + K_2 + K_3$. Thus,

$$K = 0.5\big(I_{S_1}\dot{\theta}_1^2 + m_2 V_{S_2}^2 + I_{x_2}\dot{\theta}_{x_2}^2 + I_{y_2}\dot{\theta}_{y_2}^2 + I_{z_2}\dot{\theta}_{z_2}^2 + m_3 V_{S_3}^2 + I_{x_3}\dot{\theta}_{x_3}^2 + I_{y_3}\dot{\theta}_{y_3}^2 + I_{z_3}\dot{\theta}_{z_3}^2\big)$$

where, I_{S_1} is the axial moment of inertia of link 1; $I_{x_2}, I_{y_2}, I_{z_2}$ are the axial moments of inertia of link 2 relative to corresponding coordinate axes of the system associated with link 2; $\dot{\theta}_{x_2}, \dot{\theta}_{y_2}, \dot{\theta}_{z_2}$ are the components of the angular velocity $\dot{\theta}_2$ about the same axes, i.e. $\dot{\theta}_2 = \left(\dot{\theta}_{x_2}^2 + \dot{\theta}_{y_2}^2 + \dot{\theta}_{z_2}^2\right)^{\frac{1}{2}}$; m_2 is the mass of link 2; V_{S_2} is the linear velocity of the center of mass of link 2; $I_{x_3}, I_{y_3}, I_{z_3}$ are the axial moments of inertia of link 3 relative to the corresponding coordinate axes of the system associated with link 3; $\dot{\theta}_{x_3}, \dot{\theta}_{y_3}, \dot{\theta}_{z_3}$ are the components of the angular velocity about the same axes, i.e. $\dot{\theta}_3$; m_3 is the mass of link 3; V_{S_3} is the linear velocity of the center of mass of link 3. Please note that the center of mass of link 1 is located on the rotating axis and the kinetic energy due to the linear velocity is canceled.

With regard to potential energy, we have:

$$P = P_1 + P_2 + P_3$$

with $P_1 = 0$; $P_2 = r_1 + r_2\sin(\theta_2^0)$; $P_3 = r_1 + l_2\sin(\theta_2^0) + r_3\sin(\theta_2^0 + \theta_3^0)$ where, $r_1 = l_{O_2C_1}$ is distance of the center of mass of link 1 from the joint axis O_2; $l_2 = l_{O_2O_3}$ is the length of link 2; $r_2 = l_{O_2S_2}$ is the distance of the center of mass of link 2 from the joint axis O_2; $r_3 = l_{O_3S_3}$ is the distance of the center of mass of link 1 from the joint axis O_3.

Indeed, under the given conditions, it is evident that the dynamics of the manipulator are coupled and nonlinear.

3 Dynamics Decoupling of the Manipulator

Let us carry out the dynamic decoupling of the 3R spatial manipulator by combining two distinct approaches: mass redistribution (subgroup A1) and actuator relocation (subgroup A2).

For this purpose, firstly, let us modify the design of the manipulator by placing the third actuator on the axes O_2 and coupling it with link 3 by a transmission. This transmission can be a parallelogram, a belt transmission, a gear transmission or other type of motion generation.

Figure 4b shows the modified design of the manipulator, featuring the delocalization of the third actuator and the integration of the transmission mechanism. By combining the mass redistribution and actuator relocation techniques, it is possible to achieve dynamic decoupling of the 3R spatial manipulator.

Under the provided conditions, including the delocalization of the third actuator, the kinetic energy of the manipulator can be expressed as follows:

$$K = 0.5\big[I_{S_1}\dot{\varphi}_{z_1}^2 + m_2 V_{S_2}^2 + I_{x_2}\dot{\varphi}_{x_2}^2 + I_{y_2}\dot{\varphi}_{y_2}^2 + I_{z_2}\dot{\varphi}_{z_2}^2 + m_3 V_{S_3}^2 + I_{x_3}\dot{\varphi}_{x_3}^2 + I_{y_3}\dot{\varphi}_{y_3}^2 + I_{z_3}\dot{\varphi}_{z_3}^2\big]$$

where $\boldsymbol{\varphi_i}$ (i = 1, 2, and 3) is the generalized angles defined as (Figure 5): $\boldsymbol{\varphi_1} = \dot{\boldsymbol{\theta}}_{\boldsymbol{1}}^{\boldsymbol{0}}$; $\boldsymbol{\varphi_2} = \dot{\boldsymbol{\theta}}_{\boldsymbol{1}}^{\boldsymbol{0}} + \dot{\boldsymbol{\theta}}_{\boldsymbol{2}}^{\boldsymbol{0}}$; $\boldsymbol{\varphi_3} = \dot{\boldsymbol{\theta}}_{\boldsymbol{1}}^{\boldsymbol{0}} + \dot{\boldsymbol{\theta}}_{\boldsymbol{2}}^{\boldsymbol{0}} + \dot{\boldsymbol{\theta}}_{\boldsymbol{3}}^{\boldsymbol{0}}$.

The components of the angles relative to the corresponding coordinate axes of the system are defined as follows: $\dot{\varphi}_{x_1} = \dot{\varphi}_{y_1} = 0$, $\dot{\varphi}_{z_1} = \dot{\theta}_1^0$; $\dot{\varphi}_{x_2} = \dot{\theta}_1^0 \sin(\theta_2^0)$, $\dot{\varphi}_{y_2} = \dot{\theta}_1^0 \cos(\theta_2^0)$ and $\dot{\varphi}_{z_2} = \dot{\theta}_2^0$; $\dot{\varphi}_{x_3} = \dot{\theta}_1^0 \sin(\theta_2^0 + \theta_3^0)$, $\dot{\varphi}_{y_3} = \dot{\theta}_1^0 \cos(\theta_2^0 + \theta_3^0)$ and $\dot{\varphi}_{z_3} = \dot{\theta}_2^0 + \dot{\theta}_3^0$; $\dot{\varphi}_{z_1}$, $\dot{\varphi}_{z_2}$ and $\dot{\varphi}_{z_3}$ are the actuator velocities.

$$\begin{aligned}
\dot{\varphi}_1 &= \dot{\theta}_1^0 \\
\dot{\varphi}_{x_2} &= \dot{\theta}_1^0 \sin\theta_2 \\
\dot{\varphi}_{y_2} &= \dot{\theta}_1^0 \cos\theta_2 \\
\dot{\varphi}_{z_2} &= \dot{\theta}_2^0 \\
\dot{\varphi}_{x_3} &= \dot{\theta}_1^0 \sin(\theta_2 + \theta_3) \\
\dot{\varphi}_{y_3} &= \dot{\theta}_1^0 \cos(\theta_2 + \theta_3) \\
\dot{\varphi}_{z_3} &= \dot{\theta}_3^0
\end{aligned}$$

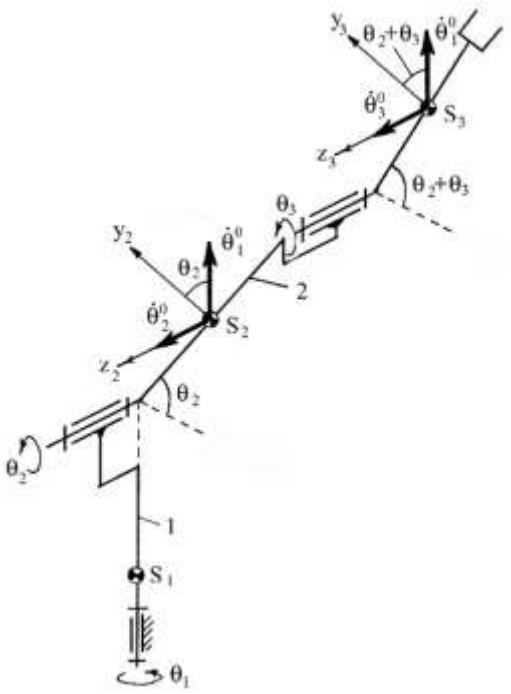

Fig. 5: Spatial serial manipulator with the absolute and relative velocities

Now, let us consider that the manipulator is statically balanced, i.e. $P = \text{const}$. It can be reached if $r_3 = 0$ and $r_2 = m_3 l_2 / m_2$, considering the location of the center of mass outside $O_2 O_3$.

Then consider that the mass distribution of the links is such that the following condition is ensured:

$$\begin{aligned}
I_{x_2} &= I_{y_2} + m_3 l_2^2 + m_2 r_2^2 = I_2^* \\
I_{x_3} &= I_{y_3} = I_3^*
\end{aligned}$$

We get

$$\begin{aligned}
\tau_1 &= (I_{z_1} + I_2^* + I_3^*)\ddot{\varphi}_{z_1} \\
\tau_2 &= (I_{z_2} + m_3 l_2^2 + m_2 r_2^2)\ddot{\varphi}_{z_2} \\
\tau_3 &= I_{z_3}\ddot{\varphi}_{z_3}
\end{aligned}$$

Consequently, the derived equations are linear and decoupled, indicating that the motion of each link can be treated independently without affecting the others. Based on these equations, it can be deduced that by minimizing the maximum values of the angular accelerations, the torques exerted on the manipulator can also be minimized. To accomplish this, the second step involves the generation of motion profiles for the links. In the context of motion generation, careful consideration should be given to the design and implementation of trajectories for the manipulator's links. By optimizing the motion profiles, it becomes possible to achieve smoother and more efficient movements,

ultimately resulting in reduced torque requirements. The goal of this second step is to develop an optimal motion generation strategy that not only ensures precise control over the manipulator's movements but also minimizes the torques exerted on the system. By effectively managing the motion profiles, the overall performance of the manipulator can be significantly improved, leading to enhanced efficiency, accuracy, and longevity of the system.

4 Motion Generation via «Bang-Bang» Profile

The path generation law, which provides the minimum of the maximum value of the acceleration is the «bang-bang» profile (Figure 6):

$$\theta(t) = \begin{cases} \theta(t_i) + 2\left(\frac{t}{t_f}\right)^2 \theta, \ \left(0 \le t \le \frac{t_f}{2}\right) \\ \theta(t_i) + \left[-1 + 4\left(\frac{t}{t_f}\right) - 2\left(\frac{t}{t_f}\right)^2\right]\theta, \ \left(\frac{t_f}{2} \le t \le t_f\right) \end{cases}$$

It is obvious that the maximal values of the angular accelerations change following the motion profile, [25]: for quantic polynomial profile $\left|\ddot{\theta}_{\max}\right| = 10\theta_f/\sqrt{3}t_f^2$ and for «bang-bang» profile $\left|\ddot{\theta}_{\max}\right| = 10\theta_f/\sqrt{3}t_f^2$. This simple comparison shows the difference between the maximum acceleration values of these two laws.

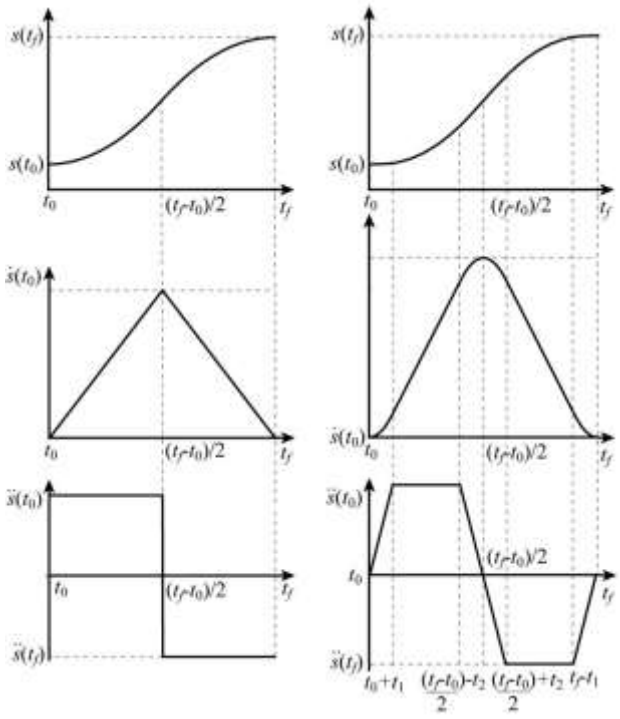

(a) «Bang-bang» law (b) Trapezoidal law

Fig. 6: «Bang-bang» and trapezoidal motion profiles

However, it is important to note that the «bang-bang» profile (Figure 6a) presented is based on theoretical considerations. In practical applications, actuators are unable to generate discontinuous efforts. Therefore, it becomes necessary to modify this motion profile by employing a trapezoidal profile (Figure 6b). As studies have shown in, [26], it appears that for given actuator parameters, the minimizations obtained in the cases of the «bang-bang» and trapezoidal profiles are very close (less than 1 %).

Indeed, the application of the «bang-bang» law in motion generation theoretically leads to a reduction of approximately 30% in the maximum value of the angular acceleration. Therefore, to minimize the maximum values of the angular accelerations and, consequently, the torques exerted on the rotating links 1, 2, and 3, it is recommended to employ the «bang-bang» profile. By reducing the angular accelerations of the manipulator's links, a corresponding decrease in the torques can be achieved.

5 Illustrative Example with CAD Simulation Results

To create a CAD model and carry out simulations via ADAMS software, a decoupled 3R spatial serial manipulator with $m_2 = 2\text{kg}$; $r_2 = 0.2\text{m}$; $m_3 = 1\text{kg}$; $l_2 = 0.4\text{m}$; $I_{z_1} = 0.6\text{kgm}^2$; $I_{z_2} = 0.3\text{kgm}^2$; $I_{z_3} = 0.14\text{kgm}^2$; $I_{x_3} = I_{y_3} = 0.1\text{kgm}^2$ was used. The initial and final values of the rotating angles θ_1, θ_2 and θ_3 are the following: $\theta_{1i} = \theta_{2i} = \theta_{3i} = 0$; $\theta_{1f} = 90°$, $\theta_{2f} = 80°$ and $\theta_{3f} = 60°$. Two types of motions for $t_f = 1\text{s}$ are simulated: 1) with fifth order polynomial profile wildly used in industrial robots; 2) «bang-bang» profile.

According to the simulation results depicted in Figure 7, Figure 8 and Figure 9, it is apparent that there is a significant reduction in torques for the two studied cases.

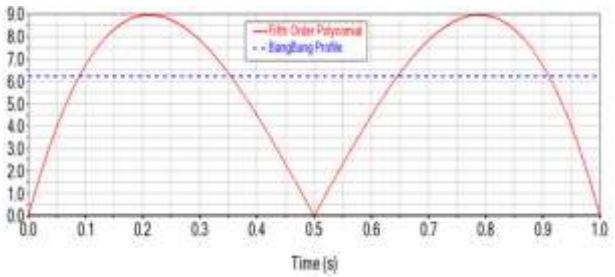

Fig. 7: Variations of torque τ_1 (Nm) for two studied cases

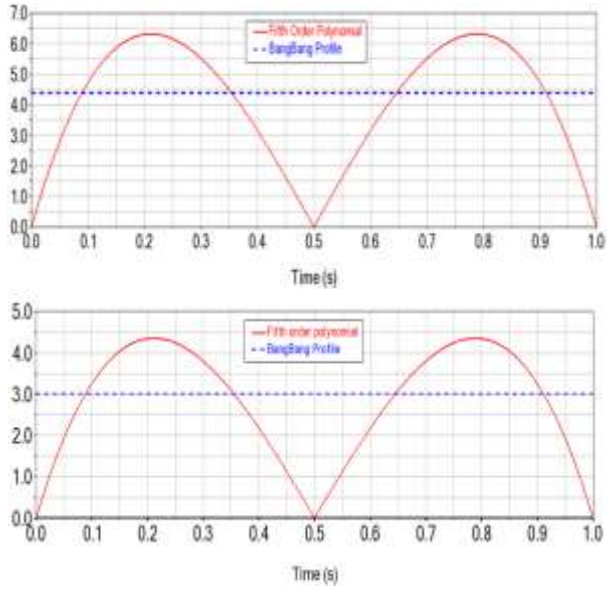

Fig. 8: Variations of torque τ_2 (Nm) for two studied cases

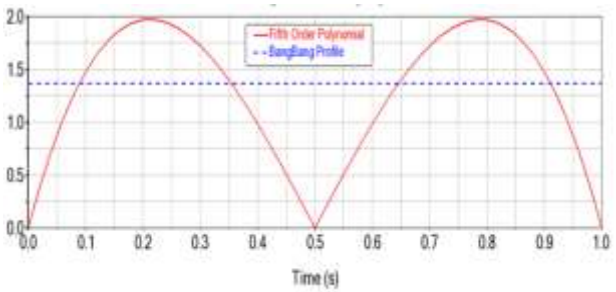

Fig. 9: Variations of torque τ_3 (Nm) for two studied cases

In the first case, where the motion is generated using the fifth order polynomial profile, and in the second case, where the motion is generated using the «bang-bang» profile, both cases exhibit a reduction in torques of up to 30.62%. These findings confirm the effectiveness of utilizing the «bang-bang» profile for motion generation in minimizing the torques exerted on the manipulator's links.

Overall, the simulation results provide quantitative evidence of the benefits of utilizing the «bang-bang» profile in terms of torque reduction, validating the effectiveness of the proposed approach in improving the manipulator's performance.

6 Error-Sensitivity Analysis of the Manipulator

Let us now carry out Sobol sensitivity analysis, [27], to reveal the sensitivity of errors of the painmeters of the manipulator. The purpose is to identify parameters' errors more affe the input torques.

According to the Sobol method, the first-order sensitivity index is stated as follows:

$$S_i = \frac{Var_{X_i}(E_{X\sim i}(Y|X_i))}{Var(Y)}$$

and total order index is given as:

$$ST_i = \frac{E_{X\sim i}(Var_{X_i}(Y|X_i))}{Var(Y)} = 1 - \frac{Var_{X\sim i}(E_{Xi}(Y|X_i))}{Var(Y)}$$

where, S_i measures the contribution of the parameter X_i to the total variance of the response. The total order index represents the total contribution (including interactions) of a parameter X_i to the total variance of the responTor to reduce the computational burden, the generally used Monte Carlo estimators are introduced here, [28]:

$$Var_{X_i}(E_{X\sim i}(Y|X_i)) \approx \frac{1}{N}\sum_{j=1}^{N} f(B)_j(f(A_B^i)_j - f(A)_j)$$

$$E_{X\sim i}(Var_{X_i}(Y|X_i)) \approx \frac{1}{2N}\sum_{j=1}^{N}(f(A)_j - f(A_B^i)_j)^2$$

where, A and B are the matrixes of all the parameters generated by the Sobol sequence, which is a uniform sampling method. A_B is the combination of the columns of matrix A and B. The accuracy of the Monte Carlo estimators depends on the number of points in every interval of parameters (more points more accurate). As mentioned above, in this case, the sensitivity of parameters to the torque 1, 2 and 3 is studied. The Sobol sequence is applied for the uniform sampling in every interval of parameters, which has ±5% error, wherein 8000 points are distributed in every interval of parameters for the sampling. The simulation results are presented in Table 1.

From the obtained results, it can be seen that I_{z_1} and I_{z_3} are the most influencing factors to the input torques 1 and 3 but for the torque 2, the parameters l_2 and m_3 are actually the most influencing factors. Thus, the most influential parameters I_{z_1}, l_2, m_3, I_{z_3} must be identified more correctly in the control system as errors in these parameters influence more on the input torques.

7 Discussion

The application of the «bang-bang» law is widely known to reduce the maximum value of acceleration. This property has been successfully utilized in previous studies, such as, [28], [29], [30]

to mitigate the impact of inertia forces on the vibration of the manipulator's base. However, applying this approach to reduce input torque presents a more challenging task due to the dynamic coupling between the degrees of freedom within the manipulator. The key to solving this problem lies in the dynamic decoupling of the manipulator. By achieving dynamic decoupling, the input torques can be linearized and dependent on only one input parameter. By utilizing this approach, a simpler control system can be implemented, as the input torque is less reliant on complex interactions between different degrees of freedom. The current study focuses on the investigation of the 3R serial spatial manipulators. However, the proposed approach can potentially be extended to other manipulators, provided that their dynamic decoupling is achievable. Using the outlined method, a decrease in input torques has been successfully attained. This was illustrated through CAD simulations.

By combining dynamic decoupling with the application of the «bang-bang» law, this study aims to simplify the manipulator's control and reduce input torques, thereby enhancing the overall efficiency of the manipulation system.

8 Conclusion

This paper considers the problem of reducing the torques in robot manipulators with decoupled dynamics. The 3R spatial serial manipulator is considered. The main objectives and findings of the study are summa-rized as follows: 1) Dynamic decoupling of the manipulator: the study successfully achieves dynamic decoupling by implementing techniques such as mass redistribution, centre of mass arrangement, and actuator relocalization. These modifications result in decoupled and linear dynamic equations for the manipulator. 2) Proportional relationship between input torques and angular accelerations: It is demonstrated that in the dynamically decoupled manipulator, the input torques are directly proportional to the input angular accelerations.

This relationship allows for simplified control and improved manageability of the manipulator. 3) Application of the «bang-bang» profile for motion generation: The proposed approach suggests using the «bang-bang» profile for motion generation, which effectively reduces the maximal values of input torques. This motion profile optimization contributes to enhanced performance and torque reduction in the manipulator. 4) Efficiency demonstrated through numerical simulations: the effectiveness of the proposed solution is illustrated through numerical simulations conducted using ADAMS software.

Table 1. Simulation results

Sobol indices						
Design parameters	Torque 1		Torque 2		Torque 3	
	S	ST	S	ST	S	ST
m_1	0	0	0	0	0	0
x_{r_1}	0	0	0	0	0	0
y_{r_1}	0	0	0	0	0	0
z_{r_1}	0	0	0	0	0	0
I_{x_1}	0	0	0	0	0	0
I_{y_1}	0	0	0	0	0	0
I_{z_1}	0.68	0.68	0	0	0	0
l_1	0	0	0	0	0	0
m_2	0.02	0.02	-0.03	0.19	0	0
x_{r_2}	0.05	0.07	0.02	0.16	0	0
y_{r_2}	0	0	0.12	0.03	0	0
z_{r_2}	0	0	0	0	0	0
y_{r_2}	0	0	0.12	0.03	0	0
z_{r_2}	0	0	0	0	0	0
I_{x_2}	0	0.18	0.07	0.03	0	0
I_{y_2}	0.03	0.01	0.01	0	0	0
I_{z_2}	0	0	0.07	0.07	0	0
l_2	0.07	0.07	0.34	0.71	0	0
m_3	0.05	0.07	0.18	0.33	0	0
x_{r_3}	0.02	0.03	0.03	0.03	0.04	0.16
y_{r_3}	0.01	0.01	0.05	0.03	-0.06	0.05
z_{r_3}	0.01	0	0	0	0	0
I_{x3}	0.05	0.05	0	0	-0.09	0.02
I_{y_3}	0.02	0.02	0	0	-0.05	0.02
I_{z_3}	0	0	0.05	0.05	0.81	0.81
l_3	0	0	0	0	0	0

These simulations validate the efficiency and benefits of the suggested approach in reducing torques and improving manipulator performance. 5) Sensitivity analysis using the Sobol method: the study also conducts a sensitivity analysis of design parameters about the input torques using the Sobol method. This analysis provides insights into the impact of different design parameters on torque

requirements and can inform future optimization efforts.

Overall, this research makes a new contribution to the advancement of torque reduction methods in manipulators with decoupled dynamics. The combination of dynamic decoupling and motion generation optimization provides new results for improving the design and control of manipulators. The primary accomplishment of this work can be summarized as follows: when designing 3R spatial manipulators, it is highly recommended to incorporate dynamic decoupling, as it greatly simplifies the control process and justifies the application of the «bang-bang» law of motion to reduce input torques.

Acknowledgement:
This study was carried out as part of Yaodong Lu's Ph.D. dissertation, with the support of the China Scholarship Council [Grant Number: 202008070129].

References:

[1] Arakelian V. (Editor), *Dynamic Decoupling of Robot Manipulators*. Springer, Switzerland, 2018.

[2] Youcef-Toumi, K., Asada, H. "The design of open-loop manipulator arms with decoupled and configuration-invariant inertia tensors," In *Proceedings of 1986 IEEE International Conference on Robotics and Automation*, pp. 2018–2026, San Francisco, California, 1986.

[3] Youcef-Toumi, K., Asada, H. "The design of open-loop manipulator arms with decoupled and configuration-invariant inertia tensors" *Journal of Dynamic Systems, Measurement, and Control*, 109(3), p.268–275, 1987.

[4] Gompertz, R. S., Yang, D. C. "Performance evaluation of dynamically linearized and kinematically redundant planar manipulators," *Robotics and computer-integrated manufacturing*, 5(4), pp. 321–331, 1989.

[5] Belyanin P.N. et al.: *Mechanical arm*. U.S. Patent 4259876, April 7, 1981.

[6] Youcef-Toumi K. "Analysis, design and control of direct-drive manipulators," Ph.D Thesis, Massachusetts Institute of Technology, Dept. of Mech. Eng., 1985.

[7] Youcef-Toumi K., Asada H. "The design of arm linkages with decoupled and configuration-invariant inertia tensors: Part II: Actuator relocation and mass redistribution," In *Proceedings of 1985 ASME, Winter Annual Meeting*, Miami, pp. 153-161, 1985.

[8] Korendyasev A. L. et al. *Manipulation Systems of Robots*. Moscow, Mashinostroyenia, 1989, p.782.

[9] Minotti, P. "Découplage dynamique des manipulateurs: propositions de solutions mécaniques, *Mechanism and Machine Theory*, 26(1), pp. 107-122, 1991.

[10] Youcef-Toumi K. "Analysis and design of manipulators with decoupled and configuration-invariant inertia tensors using remote actuation," *Transactions of the ASME. Journal of Dynamic Systems, Measurement, and Control*, 114, June, pp. 204-212, 1992.

[11] Chug Y.-H., Gang J.-G., Lee J.-W. "The Effect of actuator relocation on singularity, Jacobian and kinematic isotropy of parallel robots," In: *Proceedings of the 2002 IEEWRSJ Intl. Conference on Intelligent Robots and Systems EPFL*, Lausanne, Switzerland, October 2002, DETC2005-99532: pp. 2147-2153, 2022.

[12] Vukobratovic K.M., Stokic D.M. "Contribution to the decoupled control of large-scale mechanisms. *Automatica*," pp. 9-21, 1980.

[13] Coelho, T. A. H., Yong, L., and Alves, V. F. A. "Decoupling of dynamic equations by means of adaptive balancing of 2-dof open-loop mechanisms," *Mechanism and Machine Theory*, 39(8), pp. 871–881, 2004.

[14] Moradi, M., Nikoobin, A., and Azadi, S. "Adaptive decoupling for open chain planar robots," *Scientia Iranica: Transaction B, Mechanical Engineering*, 17(5), p.376–86, 2010.

[15] Arakelian, V., Xu, J., Le Baron, J.-P. "Mechatronic design of adjustable serial manipulators with decoupled dynamics taking into account the changing payload," *Journal of Engineering Design*, 27(11), pp. 768-784, 2016.

[16] Xu, J. Arakelian, V., Le Baron J.-P. "Dynamic decoupling of adjustable serial manipulators taking into account the changing payload," In *Proceedings of the 4th IFToMM International Symposium on Robotics and Mechatronics*, 23-25 June, Poitiers, France, pp. 313–320, 2016.

[17] Freemantle W. *Straight-line linkage*. British Patent 2741. November 17, 1803.

[18] Xu, J., Le Baron, J.-P., Arakelian, V. "Tolerance analysis of planar serial manipulators with decoupled and non-

decoupled dynamics," In *Proceedings of the 6th European Conference on Mechanism Science*, 20-23 September, 2016, Nantes, France, pp. 29–37, 2017.

[19] Herman, P. "Decoupled PD set-point controller for underwater vehicles," *Ocean Engineering*, 36(6-7), pp. 529-534, 2009.

[20] Herman, P. "Energy based indexes for manipulator dynamics improvement," *Journal of Intelligent and Robotic Systems*, 44, pp. 313–325, 2005.

[21] Herman, P. "Non-linearity evaluation and reduction for serial manipulators," *Proceedings of the Institution of Mechanical Engineers: Journal of Multibody Dynamics* – Part K, 220, pp. 283–291, 2006.

[22] Pons, J.L., Ceres, R., Jimenez, A.R., Calderon, L., Martin, J.M. "Nonlinear performance index (NPI): a tool for manipulator dynamics improvement," *Journal of Intelligent and Robotic Systems*, 18, pp. 277–287, 1997.

[23] Herman, P. "Dynamical couplings reduction for rigid manipulators using generalized velocity components," *Mechanics Research Communications*. 35(8), pp. 553-561, 2008.

[24] Arakelian, V, Geng, J., Lu, Y. "Torque minimization of dynamically decoupled 2R spatial serial manipulators via optimal motion control," *Mechanism Design for Robotics: MEDER 2021 (Mechanisms and Machine Science, 103*) pp. 20–27, 2021.

[25] Khalil, W., Dombre, E. *Modeling, Identification and Control of Robots*. Hermès, Paris, 2006.

[26] Briot, S., Arakelian, V., Le Baron, J.P. "Shaking force minimization of high-speed robots via centre of mass acceleration control," *Mech. and Mach. Theory* (57) pp; 1-12, 2012.

[27] Sobol, I.M. "Global sensitivity indices for nonlinear mathematical models and their Monte Carlo estimates," *Mathematics and Computers in Simulation* (MATCOM), Elsevier, 55(1), pp. 271-280, 2001.

[28] Saltelli, A., et al. "Variance based sensitivity analysis of model output. Design and estimator for the total sensitivity index," *Comput. Phys. Commun*., 181, pp. 259-270, 2010.

[29] Ben-Itzhak S., Karniel A. "Minimum acceleration criterion with constraints implies Bang-Bang control as an underlying principle for optimal trajectories of arm reaching movements," *Neural Computation* (2008) 20 (3), pp. 779–812, 2008.

[30] Geng J., "Design of balanced parallel manipulators with reduced center of mass acceleration," PhD thesis, INSA Rennes, France, 2021.

Contribution of Individual Authors to the Creation of a Scientific Article (Ghostwriting Policy)

- Yaodong Lu carried out the CAD simulations and edited the initial version of the manuscript.
- Vigen Arakelian was responsible for conceptualization and final editing of the manuscript.

Sources of Funding for Research Presented in a Scientific Article or Scientific Article Itself

The author Yaodong Lu's received a support of the China Scholarship Council [Grant Number: 202008070129] for the Ph.D. dissertation.

Conflict of Interest

The authors have no conflicts of interest to declare that are relevant to the content of this article.